PHOTONICS Research

On-demand design of spectrally sensitive multiband absorbers using an artificial neural network

Sunae So,[1] Younghwan Yang,[1] Taejun Lee,[1] and Junsuk Rho[1,2,3,*]

[1]Department of Mechanical Engineering, Pohang University of Science and Technology (POSTECH), Pohang 37673, Republic of Korea
[2]Department of Chemical Engineering, Pohang University of Science and Technology (POSTECH), Pohang 37673, Republic of Korea
[3]National Institute of Nanomaterials Technology (NINT), Pohang 37673, Republic of Korea
*Corresponding author: jsrho@postech.ac.kr

Received 25 November 2020; revised 12 January 2021; accepted 3 February 2021; posted 5 February 2021 (Doc. ID 415789); published 31 March 2021

We report an approach assisted by deep learning to design spectrally sensitive multiband absorbers that work in the visible range. We propose a five-layered metal-insulator-metal grating structure composed of aluminum and silicon dioxide, and we design its structural parameters by using an artificial neural network (ANN). For a spectrally sensitive design, spectral information of resonant wavelengths is additionally provided as input as well as the reflection spectrum. The ANN facilitates highly robust design of a grating structure that has an average mean squared error (MSE) of 0.023. The optical properties of the designed structures are validated using electromagnetic simulations and experiments. Analysis of design results for gradually changing target wavelengths of input shows that the trained ANN can learn physical knowledge from data. We also propose a method to reduce the size of the ANN by exploiting observations of the trained ANN for practical applications. Our design method can also be applied to design various nanophotonic structures that are particularly sensitive to resonant wavelengths, such as spectroscopic detection and multi-color applications.

https://doi.org/10.1364/PRJ.415789

1. INTRODUCTION

Metamaterial perfect absorbers (MPAs) have ultra-thin structures that can absorb almost all incident light [1,2]. This property has been exploited in several prominent applications such as thermal emitters [3], photovoltaics [4], spectroscopy [5], and sensors [6]. To achieve perfect absorption, MPAs have been developed as a variety of nano-structured devices that can control and manipulate the electromagnetic wave at the subwavelength scale. These structures are composed of either resonators [2,7] that couple to electric and magnetic fields, or of metal-insulator-metal (MIM) structures [8,9] that localize the electromagnetic fields inside the dielectric waveguide. Most proposed MPAs have one single resonant absorption peak in a single structure.

Multiband absorbers that exhibit multiple resonances in a single structure would be beneficial for spectroscopic or multi-color applications [10,11]. Therefore, approaches to integrate several resonators into a single structure have been proposed [12–14]. In these structures, each component excites a single resonance at each corresponding wavelength, and thereby yields overall multiband or broadband resonances. However, the approaches usually yield large or complex structures. In contrast, multiband absorbers can also be achieved using a relatively simple method of stacking several sets of MIM structures [15,16]. In particular, MIMs that have the structured top layers can provide much higher absorption of light, because the top structured layers can enhance the localized field inside the waveguide layer as well as the coupling of the incident light with the guided mode. Still, designing multiband absorbers for targeting multiple wavelengths of interest using MIM is not straightforward. In addition, the design process becomes more complicated for tasks that involve multiple designs, i.e., the design process must be repeated case-by-case for target tasks. This problem also applies to cases in which multiple design tasks must be applied to design general photonic devices. Efficient and flexible design methods are being sought.

Along with the rapid development of a machine learning technology, the design problem in nanophotonics has been mitigated recently with the capability of learning complex functions from the data [17–19]. These methods introduce artificial intelligence to represent the intricate functions and, thereby, to allow non-intuitive inverse designs in nanophotonics without the need to solve computationally expensive electromagnetic problems [20–25]. However, the approach that uses deep learning generally entails high computational cost to obtain

Table 1. Hyperparameters Used in the Training of Two Networks

	Design Network	Spectrum Network
Number of neurons	[202, 400, 1000, 2000, 1000, 500, 200, 5]	[5, 200, 500, 1000, 500, 200, 101]
Optimizer	Adam, weight decay 10^{-5}	Adam, weight decay 10^{-5}
Learning rate	From 10^{-5} to 10^{-4}	10^{-4}
Nonlinear activation functions	Leaky ReLU, $\alpha = 0.2$	Leaky ReLU, $\alpha = 0.2$

sufficient data for use in training and optimizing the network, i.e., the network itself, including the number of neurons and layers, should be optimized for the task at hand. Therefore, the overall computational cost easily exceeds that of other design methods for a single design. However, these up-front costs are incurred only once, so the method can provide subsequent on-demand designs within a few seconds.

This paper presents an efficient and spectrally sensitive design method that uses an artificial neural network (ANN) for multiband absorbers. A five-layered MIM grating structure is used for a multiband absorber, and its geometric parameters are designed using an ANN. An ANN is developed to design structures and focuses particularly on target resonant wavelengths. The developed ANN retrieves the geometric parameters from a given target input spectrum and spectral resonant wavelengths. The trained ANN is tested to evaluate its ability to design structures when given unseen optical properties, and then the designed structures are evaluated by finite difference time domain (FDTD) numerical simulation. The effective design capability of the developed network for multiple design tasks is investigated by achieving on-demand optical properties at various target wavelengths. We also show that the trained ANN can learn physical knowledge from the data by analyzing design results on gradually changing target wavelengths of the inputs. Finally, we demonstrate a method to reduce the size of an ANN through an observation for practical applications.

2. RESULTS AND DISCUSSIONS

A. Deep Learning Procedure

The total 12,100 pairs of grating structures and their associated reflection spectra were prepared using FDTD simulations for deep learning. The network to design a specified grating structure is composed of two ANNs: one is a design network, and one is a pre-trained spectrum network (Table 1). The design network retrieves design parameters of period (P), grating width (G_r), and each layer thickness (h_1, h_2, and h_{sub}) [Fig. 1(b)] from given inputs, and the pre-trained spectrum network evaluates the output of the design network by predicting optical properties of the retrieved design parameters. The input reflection spectrum with a wavelength of interest from 400 nm to 700 nm is discretized into 101 data points (R_1 to R_n). In optical design, the resonant wavelength of interest could be more important than the optical spectrum itself. Therefore, spectral information of resonant wavelengths [Index_1 to Index_n in Fig. 1(c)] is additionally fed into the network to achieve spectrally sensitive inverse design. The information is in binary form with a total length of 101, where 1 represents the resonant wavelength. The spectrum network is well-trained in advance, showing good agreement with the FDTD simulation results with an average mean squared error (MSE) of 0.001. The aid of the well-trained spectrum network increases the reliability and robustness of on-demand designs [21]. Overall, the two cascaded networks evaluate the discrepancies $l_{\text{design loss}}$ between the target and designed parameters, and $l_{\text{spectrum loss}}$ between the target and the designed spectrum [Eq. (1)]. The design loss is also added to improve the robustness of the network [26]. The network is trained to minimize the total loss, which is a weighted sum of two losses with the weight of $w = 0.01$. As a pre-processing of the data, the output grating parameters are divided by standard deviation of each parameter to mitigate different ranges of parameters. We adopt the batch gradient descent method with a batch size of 128, and all networks are trained on a single Nvidia GTX 1080 Ti with 11 GB memory.

$$
\begin{aligned}
l_{\text{total loss}} &= w l_{\text{design loss}} + (1 - w) l_{\text{spectrum loss}}, \\
l_{\text{design loss}} &= \frac{1}{n} \sum_{i=1}^{n=5} (D_{\text{target},i} - \hat{D}_{\text{designed},i})^2, \\
l_{\text{spectrum loss}} &= \frac{1}{n} \sum_{i=1}^{n=101} (R_{\text{target},i} - \hat{R}_{\text{designed},i})^2.
\end{aligned} \tag{1}
$$

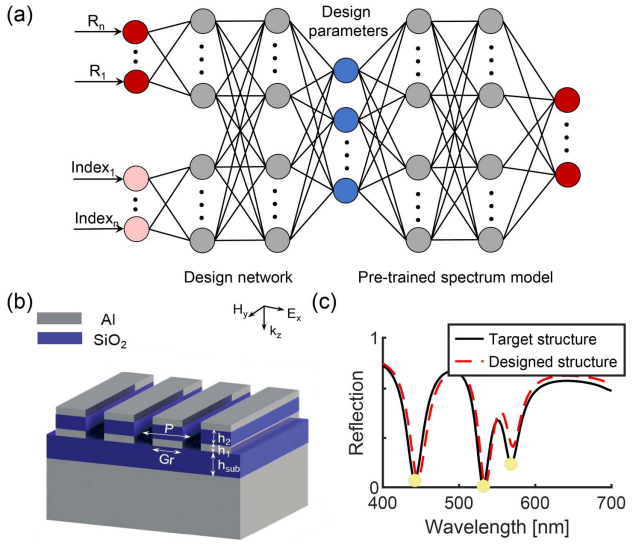

Fig. 1. Schematic of the designing grating structures for multiband absorbers. (a) A schematic of ANN for designing grating structures. The network is composed of two artificial neural networks of design network and pre-trained spectrum network. The design network both takes the input reflection spectra and resonant wavelengths, and the pre-trained spectrum network takes design parameters to evaluate the optical reflection spectra of the designed structures. (b) A schematic and (c) an example of optical property of a perfect multiband absorber under investigation. Yellow markers indicate resonant wavelengths.

B. Network Evaluation

The total data of 12,100 was split into 80% for training, 10% for validation, and 10% for testing. In every training iteration, the network was fitted on the training dataset, and then the fitted network was validated against the validation dataset. After training was complete, the trained network was evaluated against the unseen test dataset. For each given target optical property, the trained network provided a design; the parameters were then used in FDTD simulation to obtain electromagnetic responses. Figure 2(a) shows an example of the scanning electron microscope image of the designed grating structure. For a given target optical property, the FDTD simulation result and experimental result of the designed parameters show good agreement [Fig. 2(b)]. For a total of 1210 test data, the average MSE between target optical properties and designed responses was about 0.023, which shows that the network can well retrieve appropriate structures for given desired optical properties. Test examples in Fig. 2(c) show that the network can well design grating structures with high spectral accuracy.

The proposed grating MIM structure can be regarded as two cascaded MIM waveguides and, hence, can generate various electromagnetic resonances depending on structural parameters. For example, electric displacement in metal layers of the MIM structure can form a loop and, hence, generate magnetic resonance that amplifies strong electromagnetic absorption at resonant wavelengths. To analyze mechanisms of multiple resonances in the structure, we calculated the magnetic field distributions and electric displacements at the resonant wavelengths [Fig. 3(a)]. Figures 3(b)–3(d) clearly show that the magnetic fields are strongly localized in the waveguide region. The electric displacements in the structure (white arrows) form closed loops (green circles), generating strong magnetic

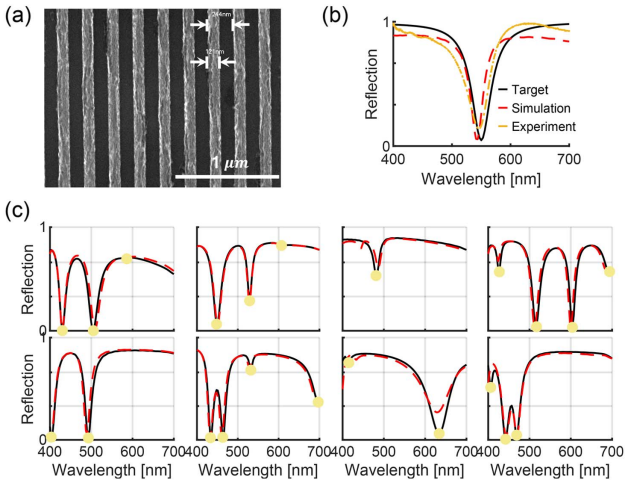

Fig. 2. (a) Scanning electron microscope image of a designed grating structure with a scale bar of 1 μm. (b) Target reflection spectrum (black solid line) and designed optical properties obtained from the FDTD simulation (red dotted line) and experiment (yellow dotted line). Grating parameters with $[P, G_r, h_1, h_2, h_{sub}]$ = [245 nm, 120 nm, 42 nm, 113 nm, 195 nm] are designed by the network. (c) Examples of test results are shown. Black solid lines and red dotted lines are the input and target reflection spectra, respectively, and yellow markers are indexed resonant wavelengths.

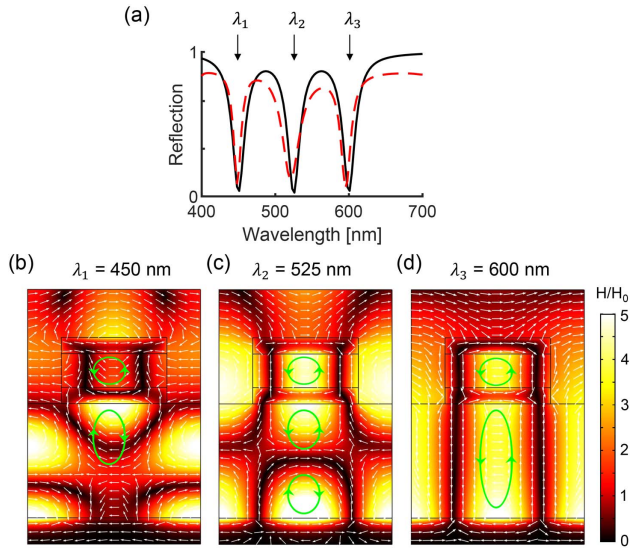

Fig. 3. (a) Target (black solid line) and designed reflection spectrum. Magnetic field distribution (color maps) and electric displacement (arrow surfaces) at the resonant wavelengths of (b) 450 nm, (c) 525 nm, and (d) 600 nm.

resonances. At the wavelength of $\lambda_1 = 450$ nm, electric displacements in two SiO_2 waveguide regions are symmetric with respect to the second Al layer. On the other hand, electric displacements in two SiO_2 waveguide regions are antisymmetric with respect to the second Al layer at the wavelengths of $\lambda_2 = 525$ nm and $\lambda_3 = 600$ nm. At the wavelengths of $\lambda_3 = 600$ nm and $\lambda_2 = 525$ nm, the first and second orders of Fabry–Perot modes are generated inside the second SiO_2 waveguide region. Overall, the cascaded MIM grating structures allow many interesting optical responses at

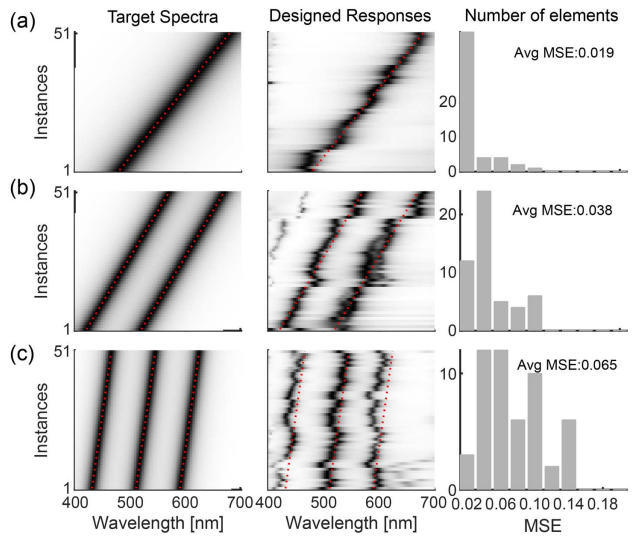

Fig. 4. Design of multiband absorbers with (a) single, (b) double, and (c) triple resonances. The first column shows the target input spectra, and the second column shows the designed responses. The red lines indicate target resonant wavelengths. The third column shows the histogram of the MSE for a total of 51 input spectra. The insets show the average MSE of the test input.

various resonant wavelengths; for this reason, the proposed structures are compatible with design by deep learning. Design approaches that use deep learning usually entail a very high initial computational cost to obtain large amounts of data, but the trained network can be used repeatedly to design various structures. Therefore, for multiple design tasks that target various resonant wavelengths, the trained network can very quickly design structural parameters that have the desired optical properties.

To demonstrate the ANN's capability for multiple design tasks, we tested our network with various target reflection spectra drawn with Lorentzian-shaped resonances (Fig. 4). We aimed to design various absorbers that had single [Fig. 4(a)], double [Fig. 4(b)], and triple [Fig. 4(c)] resonances. For each multiband absorber, 51 instances of optical properties with different resonant wavelengths were used as desired target inputs. For a total of 153 target optical properties, the designed responses show very good agreement. In particular, the optical properties are well represented in the target wavelength regions due to the additional inputs of the target resonance wavelengths. The MSE histograms (Fig. 4) show the statistical error distribution of a dataset having 10 bins with an interval of 0.02. The histogram counts the number of cases with MSE that fall into each range out of a total of 51 cases. Overall, the average MSE tended to increase as the number of resonances was increased due to the difficulty of targeting multiple resonances. Still, results clearly show that the ANN has highly generalizable capability to design various target spectra. The network performance for designing multiband absorbers could be improved if more data on multiband spectra are added to the training data.

To investigate the effect of additional input information, we also trained the network without the spectral information of resonant wavelengths (Fig. 5). The network uses all other parameters the same as those used in the main text, except that the network only takes the reflection spectrum as input. Without resonant wavelength information (the middle of Fig. 5), the predicted optical properties of the designed structures can well mimic the overall behaviors of the target optical properties, but resonant wavelengths deviate from the target wavelengths (red dotted lines) resulting in poor spectral accuracy. On the other hand, with the resonant wavelength information, the network can show much higher spectral accuracy (the right of Fig. 5).

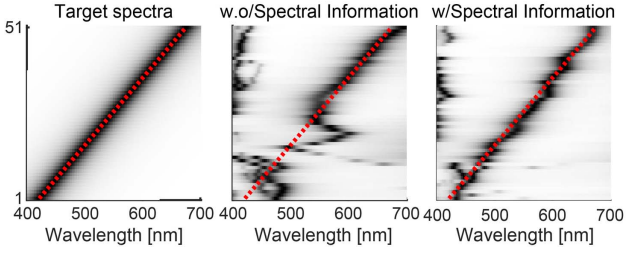

Fig. 5. Comparison between two networks fed with and without spectral resonant wavelengths. The left is the target input spectra; the middle and the right are the predicted response of the networks without and with spectral information, respectively. The red lines are target resonant wavelengths.

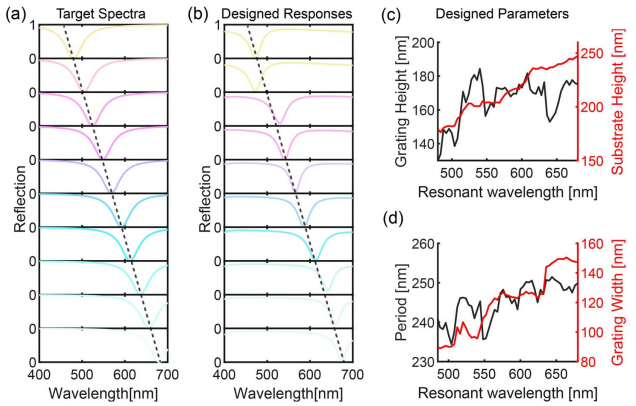

Fig. 6. Analysis on output parameters for gradually changing target resonant wavelengths. (a) Target spectra with gradually changing resonant target wavelengths and (b) corresponding designed responses. For given varying input spectra, the designed parameters of (c) grating height and substrate height and (d) period and grating width.

The design capability of the trained ANN was further investigated by analyzing the output parameters as the target resonant wavelengths were gradually changed (Fig. 6). For gradually changing the target resonant wavelength from 480 nm to 680 nm of the single resonant absorber [Fig. 6(a)], ANN successfully designed structures that can reproduce the desired properties [Fig. 6(b)]. Figures 6(c) and 6(d) show the designed parameters for given inputs. Interestingly, when the target resonant wavelength was redshifted, the designed substrate heights tended to increase, whereas the designed total grating heights rarely changed. In addition, the periods were almost unchanged at ~245 nm, but the grating widths increased continuously. These tendencies correspond to our physical intuitions and knowledge, i.e., it is well known that increasing the height of the insulator inside the MIM structure will lead to the redshifted electromagnetic resonances. Also, the increased grating width leads to an increased effective refractive index of the waveguide structure resulting in redshift of the resonant wavelength. Therefore, these results suggest that the ANN can learn physics by analyzing data.

C. Network Pruning

We demonstrate an approach to prune the ANN by eliminating unnecessary neurons through observation of the trained network. It has been known that building large ANNs can generally perform better on a variety of tasks, but it is also more expensive to use. Therefore, it is important to reduce the size of networks while minimizing performance degradation. ANN pruning is a method of compressing network size by removing weights [27–29]. Here, we demonstrate pruning the ANN through observation. After the network was trained, we visualized the trained values of the weights connecting neurons in the previous input layer (x axis) to neurons in the output layer (y axis) (Fig. 7). Interestingly, we observed that some weights linking between two neurons are almost zero [white in Fig. 7(a)]. For example, all weights connecting from all neurons in layer 2 (L2) to the first neuron in layer 3 (L3) are zero (the first white horizontal line in L3), so the neuron is turned off.

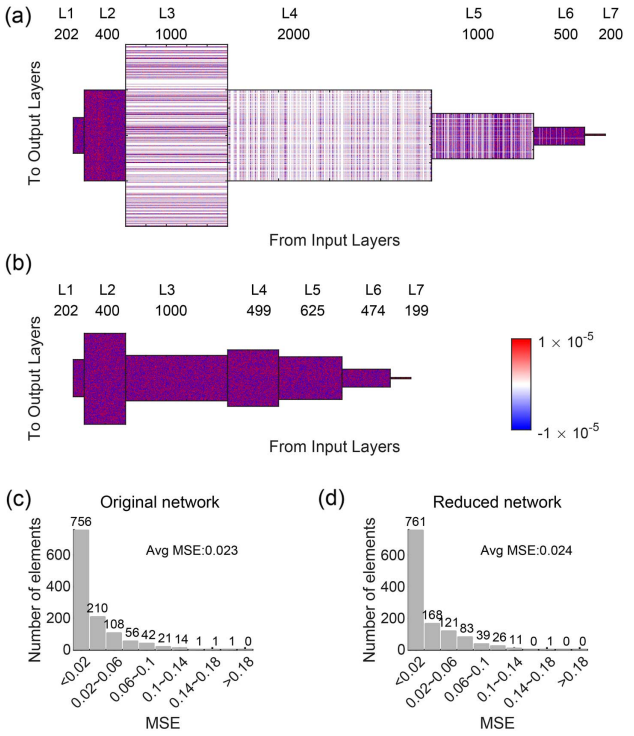

Fig. 7. Network pruning results. Visualization of the trained weights in (a) the original network and (b) the pruned network. For each layer ($Ln, n = 1, 2, \ldots, 7$), the number of neurons is indicated. MSE histogram of the test data for (c) the original network and (d) the pruned network.

It means that the neuron did not receive any information from all neurons in the previous layer and, consequently, did not transmit any information to the next layer (the first white vertical line in L4). This implies that the neuron did not participate in learning, so layer 3 has more neurons than necessary. Therefore, we counted the number of such turned-off neurons in each layer and removed the neurons to reduce the total size of the network. By reducing the size of the network, the number of trainable parameters is reduced from about 5 million to 1.6 million (Table 2). Not surprisingly, despite the significant network compression, the pruned network retains the design capability similar to the original network in the MSE histogram of the test data [Figs. 7(c) and 7(d)]. In addition, the pruned network also enables efficient multiple design tasks for various user-drawn spectra (Fig. 8). These results suggest that the network can be pruned through observation of the trained weights. The proposed network method could be applied to any other research fields that use ANN.

Table 2. Number of Neurons in Each Layer

Layer	1	2	3	4	5	6	7	Total
Original	202	400	1000	2000	1000	500	200	5055905
Reduced	202	400	1000	499	625	474	199	1651642

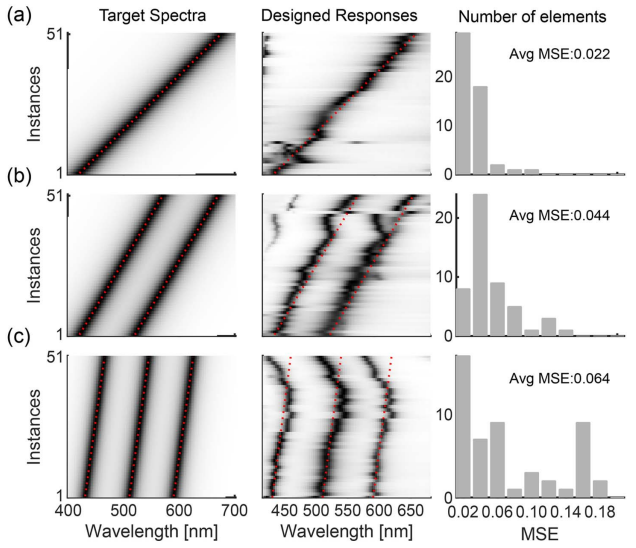

Fig. 8. Design of multiband absorbers with (a) single, (b) double, and (c) triple resonances using the reduced network. The first column shows target input spectra, and the second column shows the designed response. The red lines indicate target resonant wavelengths. The third column shows the histogram of the MSE for a total of 51 input spectra.

3. CONCLUSION

We have proposed a method that uses deep learning to design spectrally sensitive multiband absorbers. By feeding additional spectral information of resonant wavelengths, the developed ANN achieved a highly robust and accurate design of multiband absorbers. We have also analyzed the results of the designed outputs when the resonant wavelength was gradually changed. For gradually redshifting inputs, the designed parameters of the substrate height and period tended to increase, in correspondence to physical intuition. The results suggest that the trained network can well grasp and learn physics by analyzing data. We envision that this can also be applied to other nanophotonic problems and may solve complex light–matter interactions that are even beyond our knowledge. Finally, we proposed a systematic method that uses observation of the trained network to guide its pruning. The method is expected to significantly reduce the computational cost involved in network reduction. The method could be extended to other research fields that use ANNs. In this study, we considered designing one structure for one given spectrum, but it is worth noting that multiple candidates could be designed by using deep learning algorithms for multi-output regression. We believe considering several design candidates would be beneficial for fabrication when the target design becomes much more complex.

Funding. National Research Foundation of Korea (NRF-2018M3D1A1058998, NRF-2019R1A2C3003129, CAMM-2019M3A6B3030637, NRF-2019R1A5A8080290, NRF-2020K1A3A1A21024374); Ministry of Education (NRF-2017H1A2A1043322, NRF-2019H1A2A1076295).

Acknowledgment. Y. Y. acknowledges a fellowship from the Hyundai Motor Chung Mong-Koo Foundation.

Disclosures. The authors declare that there are no conflicts of interest related to this paper.

REFERENCES

1. N. Engheta, "Thin absorbing screens using metamaterial surfaces," in *IEEE Antennas and Propagation Society International Symposium* (IEEE, 2002), pp. 392–395.
2. N. I. Landy, S. Sajuyigbe, J. J. Mock, D. R. Smith, and W. J. Padilla, "Perfect metamaterial absorber," Phys. Rev. Lett. **100**, 207402 (2008).
3. M. Diem, T. Koschny, and C. M. Soukoulis, "Wide-angle perfect absorber/thermal emitter in the terahertz regime," Phys. Rev. B **79**, 033101 (2009).
4. A. Vora, J. Gwamuri, N. Pala, A. Kulkarni, J. M. Pearce, and D. Ö. Güney, "Exchanging ohmic losses in metamaterial absorbers with useful optical absorption for photovoltaics," Sci. Rep. **4**, 4901 (2014).
5. F. B. Barho, F. Gonzalez-Posada, M. Bomers, A. Mezy, L. Cerutti, and T. Taliercio, "Surface-enhanced thermal emission spectroscopy with perfect absorber metasurfaces," ACS Photon. **6**, 1506–1514 (2019).
6. N. Liu, M. Mesch, T. Weiss, M. Hentschel, and H. Giessen, "Infrared perfect absorber and its application as plasmonic sensor," Nano Lett. **10**, 2342–2348 (2010).
7. H. Tao, C. Bingham, D. Pilon, K. Fan, A. Strikwerda, D. Shrekenhamer, W. Padilla, X. Zhang, and R. Averitt, "A dual band terahertz metamaterial absorber," J. Phys. D **43**, 225102 (2010).
8. J. Hao, J. Wang, X. Liu, W. J. Padilla, L. Zhou, and M. Qiu, "High performance optical absorber based on a plasmonic metamaterial," Appl. Phys. Lett. **96**, 251104 (2010).
9. P. Bouchon, C. Koechlin, F. Pardo, R. Hadar, and J.-L. Pelouard, "Wideband omnidirectional infrared absorber with a patchwork of plasmonic nanoantennas," Opt. Lett. **37**, 1038–1040 (2012).
10. K. Chen, R. Adato, and H. Altug, "Dual-band perfect absorber for multispectral plasmon-enhanced infrared spectroscopy," ACS Nano **6**, 7998–8006 (2012).
11. J. Xu, Z. Zhao, H. Yu, L. Yang, P. Gou, J. Cao, Y. Zou, J. Qian, T. Shi, Q. Ren, and Z. An, "Design of triple-band metamaterial absorbers with refractive index sensitivity at infrared frequencies," Opt. Express **24**, 25742–25751 (2016).
12. J. W. Park, P. Van Tuong, J. Y. Rhee, K. W. Kim, W. H. Jang, E. H. Choi, L. Y. Chen, and Y. Lee, "Multi-band metamaterial absorber based on the arrangement of donut-type resonators," Opt. Express **21**, 9691–9702 (2013).
13. Y. Ma, Q. Chen, J. Grant, S. C. Saha, A. Khalid, and D. R. Cumming, "A terahertz polarization insensitive dual band metamaterial absorber," Opt. Lett. **36**, 945–947 (2011).
14. S. Liu, H. Chen, and T. J. Cui, "A broadband terahertz absorber using multi-layer stacked bars," Appl. Phys. Lett. **106**, 151601 (2015).
15. Z. Zhang, Z. Yu, Y. Liang, and T. Xu, "Dual-band nearly perfect absorber at visible frequencies," Opt. Mater. Express **8**, 463–468 (2018).
16. G. Dayal and S. A. Ramakrishna, "Design of multi-band metamaterial perfect absorbers with stacked metal–dielectric disks," J. Opt. **15**, 055106 (2013).
17. W. Ma, Z. Liu, Z. A. Kudyshev, A. Boltasseva, W. Cai, and Y. Liu, "Deep learning for the design of photonic structures," Nat. Photonics **15**, 77–90 (2021).
18. K. Yao, R. Unni, and Y. Zheng, "Intelligent nanophotonics: merging photonics and artificial intelligence at the nanoscale," Nanophotonics **8**, 339–366 (2019).
19. S. So, T. Badloe, J. Noh, J. Rho, and J. Bravo-Abad, "Deep learning enabled inverse design in nanophotonics," Nanophotonics **9**, 1041–1057 (2020).
20. J. Peurifoy, Y. Shen, L. Jing, Y. Yang, F. Cano-Renteria, B. G. DeLacy, J. D. Joannopoulos, M. Tegmark, and M. Soljačić, "Nanophotonic particle simulation and inverse design using artificial neural networks," Sci. Adv. **4**, eaar4206 (2018).
21. D. Liu, Y. Tan, E. Khoram, and Z. Yu, "Training deep neural networks for the inverse design of nanophotonic structures," ACS Photon. **5**, 1365–1369 (2018).
22. S. So, J. Mun, and J. Rho, "Simultaneous inverse design of materials and structures via deep learning: demonstration of dipole resonance engineering using core–shell nanoparticles," ACS Appl. Mater. Interfaces **11**, 24264–24268 (2019).
23. Z. Liu, D. Zhu, S. P. Rodrigues, K.-T. Lee, and W. Cai, "Generative model for the inverse design of metasurfaces," Nano Lett. **18**, 6570–6576 (2018).
24. S. So and J. Rho, "Designing nanophotonic structures using conditional deep convolutional generative adversarial networks," Nanophotonics **8**, 1255–1261 (2019).
25. Y. Kiarashinejad, M. Zandehshahvar, S. Abdollahramezani, O. Hemmatyar, R. Pourabolghasem, and A. Adibi, "Knowledge discovery in nanophotonics using geometric deep learning," Adv. Intell. Syst. **2**, 1900132 (2020).
26. W. Ma, F. Cheng, and Y. Liu, "Deep-learning-enabled on-demand design of chiral metamaterials," ACS Nano **12**, 6326–6334 (2018).
27. J. Frankle and M. Carbin, "The lottery ticket hypothesis: finding sparse, trainable neural networks," arXiv:1803.03635 (2018).
28. D. Blalock, J. J. G. Ortiz, J. Frankle, and J. Guttag, "What is the state of neural network pruning?" arXiv:2003.03033 (2020).
29. M. Babaeizadeh, P. Smaragdis, and R. H. Campbell, "Noiseout: a simple way to prune neural networks," arXiv:1611.06211 (2016).